Chapter 7

The New Use of Diffusion Theories for the Design of Heat Setting Process in Fabric Drying

Ralph Wai Lam Ip and Elvis Iok Cheong Wan

Additional information is available at the end of the chapter

http://dx.doi.org/10.5772/48484

1. Introduction

Hot air impingement is one of the most widely used methods for material drying. It is also the most traditional drying approach used in industrial process for various kinds of material, such as wood, paper, food, medicine and construction materials. Many research studies have been carried out to see how it is effectively used to process different types of material, and how it is implemented into the design of heat setting machines, such as spray dryers, conveyor dryers, tunnel dryers, fluidized bed dryers and drum dryers.

To study hot air impingement in textile and clothing industries, modeling of porous type fabric drying process would be the key study area. The heat and mass transfer principles are used as tools to assist with the investigation of the hot air impingement mechanism. The mechanism is usually treated as a mass transfer process of the moisture content from the porous material to the impinging air. The transfer of moisture content from the fabric material to the hot air stream is due to a heat transfer process under an in-equilibrium condition. The change of water phases is traditionally described by linear heat transfer equations. As a matter of fact, the driving force in the internal structure of porous materials is not a simple direct proportional relationship between energy exchange and the phase change of the interacting substances, i.e. air and water. Therefore non-linear analytical models based on the physical properties of fabrics will be proposed in this study to provide better simulation results. In the models, the parameters for modeling will be empirically determined and used to describe the drying phenomenon down to microscopic levels. The descriptions will involve the physical and mechanical properties of the drying materials such as mass density, flow viscosity, thermal conductivity, diffusion properties, cohesive properties and flow kinetics. Ip and Wan (2011) have suggested the strategies of using analytical techniques to determine the modeling parameters, and these methods will be investigated in greater depth in this research.

2. Three periods of a fabric drying cycle

Fabric is usually dried up for the purposes of storing or setting. Using thermal energy to dry up and perform setting has been the most traditional and effective method. In this study, heated air is used as a processing agent. Its physical properties will be changed in the gaining of moisture and the loss of thermal energy. The moisture in the fabric will change to vapor after gaining energy from air to create a mass transfer process. The reduction of moisture and increase of fabric temperature is a complicated heat/mass transfer process. Merely using linear conductive and convective heat transfer equations to model the process seems to be inadequate. Diffusion theories are therefore suggested to present the details of the drying process.

"Preheating", "Constant drying" and "Falling drying" are the three periods of a fabric drying cycle as shown in Fig. 1. In the preheating period, most thermal energy is absorbed by water on the fabric surface because air is a poor thermal conductor. The mass transfer rate of water is not high in this period. When more thermal energy is absorbed, water on the fabric surface will change to vapor by evaporation at a rapid mass transfer rate. The water loss rate will keep constant depending upon the air temperature, velocity and atmospheric pressure. As the mass transfer rate of water is constant in this period, it is labeled as constant drying period. While the moisture content in the fabric is going down from the initial θ_i to critical moisture content θ_k, the moisture on the fabric surface starts to separate and form dry/wet regions. Diffusion will appear at the dry/wet regions to form the falling drying period. Diffusion is a slow mass transfer process in comparison with evaporation happened at the second period, and the water transfer rate is correspondingly decreased to form a non-linear drying result until reaching the final moisture content at θ_o.

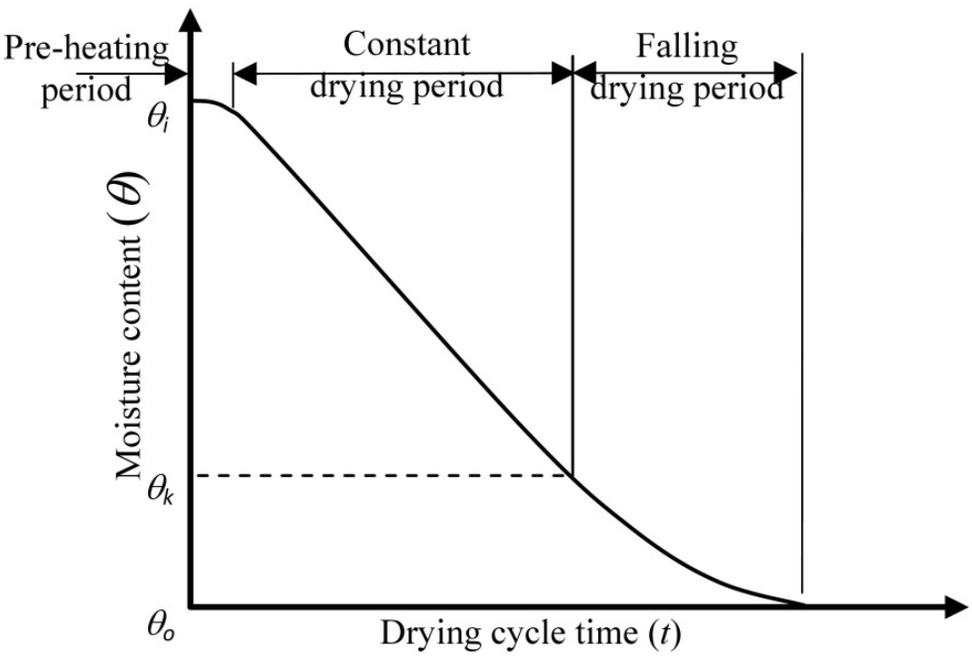

Figure 1. A typical fabric drying curve shows the three drying periods

Kowalski et al. (2007) has employed partial differentiation and numerical analysis tools to present thermo-mechanical properties of a drying process for porous materials. However, the modeling process is computational intensive and time consuming. It seems impractical to be used in the industrial drying process because a quick response is always needed to manage numerous varying conditions. The concept of using analytical approaches to model drying processes for fruits and sugar has been proved (Khazaei et al., 2008). However, its performance heavily relies upon the sample data and the reliability of the assumptions. The scopes of the research are therefore having rooms to improve the inadequacy. Objectives of the research are to explore and develop robust analytical models that can effectively simulate the characteristics of hot air impingement process for porous fabrics of different textile properties.

2.1. Research objectives

The research objectives in the Chapter are:

- to investigate how to present the drying characteristics of porous type fabric using non-linear analytical models,
- to evaluate the performance of the models in the simulation of drying process, and
- to comment their accuracies in the modeling of different fabric types under various air setting conditions.

In this research, four non-linear analytical models will be studied. The modeling parameters for the models will be empirically determined. The performance of the model will be examined through a careful comparison of testing results. A drying test will be set up to assist the determination of the modeling parameters, and evaluate the performance of the developed models.

2.2. Equations for moisture flow through control volume

Using the approach of control volume to the describe characteristics of moisture flow in porous materials would be close to the phenomenon of fabric drying (Kowalski, 2003). The total mass of the constituents within the control volume will remain unchanged when the porous fabric volume shrinks or otherwise. A set of mass balance equations for each individual constituent, i.e. water, vapor and air in a drying process is given as:

$$\rho^s \dot{X}^l = -div\, W^l + \psi^l \tag{1}$$

$$\rho^s \dot{X}^v = -div\, W^v + \psi^v \tag{2}$$

$$\rho^s \dot{X}^a = -div\, W^a \tag{3}$$

where ρ is partial mass density, $\dot{X}$ is mass content change rate, ψ is phase transition rate, s is solid fabric, l is liquid phase of water, v is vapor phase of water and a is air. The mass balance Equations (1) – (3) provides a platform for further investigation of moisture content change in a fabric drying process.

2.3. Boundary conditions for the period of constant drying

The water evaporated inside fabric material is much less than that on the boundary surface in the constant drying period. Assuming that the mass flux W of water vapor and air are negligible in this period, the relationship can be given as:

$$W^v = W^a = 0 \tag{4}$$

Then, the mass balance Equations (1) – (3) can be rewritten for the calculation of moisture content in the period of constant drying and give:

$$\rho^s \dot{X}^l = -div\, W^l + \psi^l \tag{5}$$

$$\rho^s \dot{X}^v = \psi^v << \rho^s \dot{X}^l \tag{6}$$

$$\rho^s \dot{X}^a = 0 \tag{7}$$

Equation (5) shows the phase transition of water inside the fabric. Equations (6) and (7) show the phase transition of vapor and air respectively inside the fabric.

2.4. Boundary conditions for the period of falling drying

When the fabric moisture content falls to the critical point at θ_k, meniscoidal water droplets will recede and the drying rate is slowing down until completely dry. The characteristics of fabric drying at this period could be divided into the hygroscopic and non-hygroscopic states, thus, the heat/mass transfer in this period is getting complex. At the initial stage of falling drying, the fabric is fully saturated and water flows in the form of liquid fluxes mainly due to capillary action. Air pockets gradually form at the second stage to replace some of the moisture to form small air bubbles inside the fabric pores. With further drying, the moisture decreases and the size of air bubbles considerably increases that could reduce the rate of heat transfer. As a result, the heat/mass transfer rate is correspondingly reduced since the thermal resistance of air is much higher than water. The drying cycle stops at the tertiary stage when moisture in the hygroscopic regions is totally removed, and a uniform non-hygroscopic property fabric is formed. The mass balance Equations (1) – (3) for the falling drying is rewritten to give:

$$\rho^s \dot{X}^l = \psi^\alpha \tag{8}$$

$$\rho^s \dot{X}^v = -div\, W^v + \psi^\alpha \tag{9}$$

$$\rho^s \dot{X}^a = -div\, W^a \tag{10}$$

where α in Equations (8) and (9) are all the constituents in the fabric.

2.5. Calculation of mass fluxes

The mass flux of water in Equation (5) at the constant drying period is given as:

$$W^l = -\wedge^l \left[\left(\frac{\partial \mu^l}{\partial T^l} \right) T^l + \left(\frac{\partial \mu^l}{\partial \theta^l} \right) \theta^l + \left(\frac{\partial \mu^l}{\partial X^l} \right) X^l - g \right] \tag{11}$$

$$C^l = \left(\frac{\partial \mu^l}{\partial \theta^l} \right) \tag{12}$$

In Equation (11), $\wedge$ is the coefficient of water diffusivity, μ is chemical potential of water, θ is relative moisture content, T is absolute temperature and g is gravitational acceleration. The equation shows the relationship between water mass flux W^l and the gradients of temperature, volume fraction and mass fraction. The water movement in the fabric is largely due to capillary forces and gravitational force at the constant drying period. C^l is the moisture coefficient related to the moisture cohesive force in the fabric. The mass flux of vapor in Equation (9) for the falling drying period is given as:

$$W^v = -\wedge^v \left[\left(\frac{\partial \mu^v}{\partial T^v} \right) T^v + \sum \left(\frac{\partial \mu^v}{\partial \theta^v} \right) \theta^v \right] \tag{13}$$

$$C^v = \left(\frac{\partial \mu^v}{\partial \theta^v} \right) \tag{14}$$

The generation of moisture is due to phase transition of water into vapor, in which, the efflux of vapor is significant. The coefficient C^v for water vapor could be experimentally determined.

3. Fabric drying tests

A series of experiments were conducted to measure the drying characteristics of a group of fabric samples. Cotton is the major studying material in the tests as it is used most widely in clothing industry. The objectives of the experimental tests are to examine the drying characteristics of the fabrics under different boundary conditions, such as fabric texture, density, thickness, air temperature and impingement velocity.

3.1. Drying test set up

Six cotton fabric samples were examined. The samples were labeled from A to F, and their properties are listed in Table 1.

The set up as shown in Fig. 2 is an air heater providing hot air stream for each drying test. The temperature and speed of the impinging air are adjustable to provide different boundary conditions for the study. Disc-shaped fabric samples of 100 cm^2 in area are mounted on a polystyrene backing plate with wire gauze facing the impinging hot air.

Fabric sample	Fabric texture	Yarn structure	Density (g/m³)	Thickness (mm)
A	Plain knitted	20 s/2	224.4	0.6594
B	Plain knitted	32 s/1	147.7	0.4363
C	Plain knitted	20 s/2	271.0	0.7769
D	Plain weaved	-	182.0	0.5638
E	Plain knitted	20 s/1	193.0	0.5025
F	Plain knitted	32 s/2	200.0	0.6188

Table 1. The properties of the fabric samples for drying tests

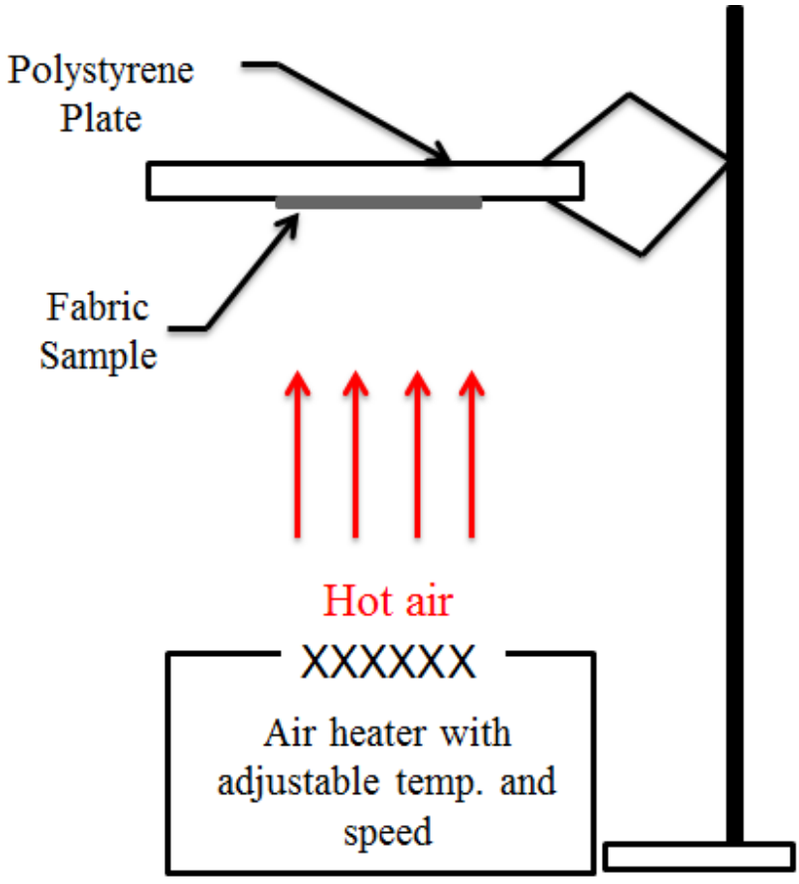

Figure 2. Schematic diagram of the drying test setup

In the tests, each fabric sample was being dried under eight conditions as listed in Table 2. The fabric weight was measured by an electronic balance every 30 seconds of drying under different setting conditions. The repeated drying and weight measurement procedures were conducted until all the moisture in the fabric samples was removed. The same testing procedures were repeated for all the fabric samples as given in Table 1.

Setting condition	Air temperature (℃)	Impinging velocity (m/s)
1	80.0	1.48
2	81.5	1.45
3	86.5	1.43
4	54.0	1.10
5	55.5	1.15
6	54.0	1.02
7	57.0	1.41
8	58.0	1.46

Table 2. The air setting conditions of drying tests for the six fabric samples

3.2. Results and discussions of the drying tests

Fig. 3 shows testing results from the six fabric samples under air setting condition 1 as listed in Table 2. The normalized water contents instead of the absolute values recorded from the tests were used in order to compensate the variation of fabric weight among the six samples.

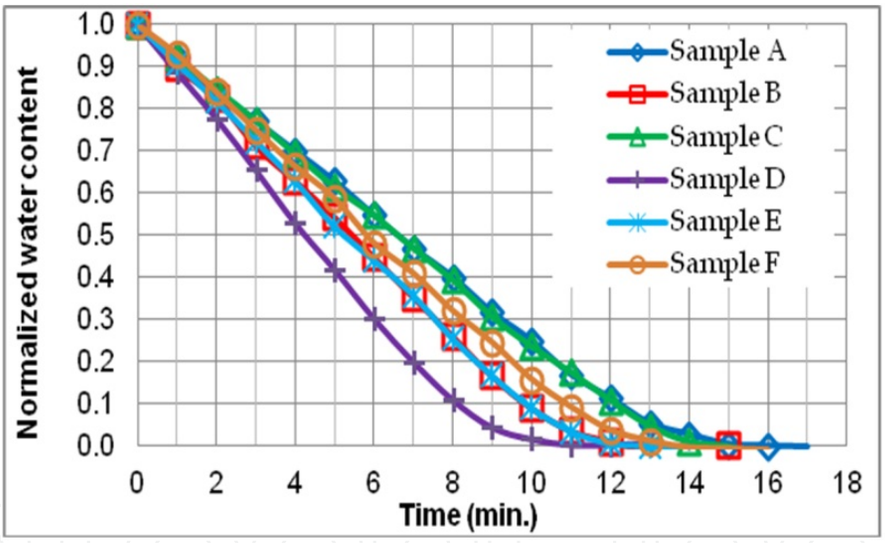

Figure 3. Drying curves for the six fabric samples under air setting condition 1

The testing results as illustrated in Fig. 3 for the tested fabrics have shown the relationships among water content, fabric density, texture, air temperature and impingement velocity. Their relationships are discussed in the following sections.

3.2.1. Drying rate versus fabric texture

Table 3 lists the results of four fabric samples tested under the air setting conditions of 1, 4, 6 and 8 as listed in Table 2. Among the tested samples, sample D is weaved fabric and the others are knitted fabrics. The drying rate of sample D is the highest among the others at the constant drying period.

	Sample B - Plain knitted		**Sample D** - Plain weaved	
Air setting condition	**1/Drying time (min^{-1})**	**Drying rate at constant drying period (g/min)**	**1/Drying time (min^{-1})**	**Drying rate at constant drying period (g/min)**
1	0.083	0.439	0.100	0.462
4	0.080	0.383	0.100	0.395
6	0.095	0.392	0.083	0.398
8	0.065	0.281	0.065	0.287
	Average drying rate = 0.374 g/min		Average drying rate = 0.386 g/min	
	Sample E - Plain knitted		**Sample F -** Plain knitted	
1	0.083	0.431	0.077	0.426
4	0.067	0.304	0.057	0.323
6	0.063	0.349	0.065	0.385
8	0.061	0.290	0.056	0.302
	Average drying rate = 0.344 g/min		Average drying rate = 0.359 g/min	

Table 3. Drying rate of the four tested samples with different fabric texture

3.2.2. Drying rate versus fabric density and thickness

Table 4 lists the testing results of two selected fabric samples A and C with same texture, yarn structure and different density and thickness under the air setting conditions of 1, 4, 6 and 8.

	Sample A - 224.4 g/m^3, 0.6594 mm		**Sample C** - 271 g/m^3, 0.7769 mm	
Air setting	**1/Drying time (min^{-1})**	**Drying rate at constant drying period (g/min)**	**1/Drying time (min^{-1})**	**Drying rate at constant drying period (g/min)**
1	0.071	0.416	0.067	0.443
4	0.063	0.407	0.063	0.391
6	0.065	0.378	0.053	0.396
8	0.047	0.281	0.044	0.289
	Average drying rate = 0.371 g/min		Average drying rate = 0.380 g/min	

Table 4. Drying rates of samples A and C for different air setting conditions

The results listed in Table 4 show a similar result at the constant drying for the fabrics with different density and thickness, but same texture and yarn structure.

3.2.3. Drying rate versus air temperature

Table 5 lists the results of the drying rate for all fabric samples tested under air setting conditions 1 and 8 with similar impingement velocity at 1.47 m/s and different temperature.

	Sample A		Sample B		Sample C	
Temp. (°C)	1/time (min^{-1})	Drying rate (g/min)	1/time (min^{-1})	Drying rate (g/min)	1/time (min^{-1})	Drying rate (g/min)
58	0.047	0.281	0.065	0.281	0.044	0.289
80	0.071	0.416	0.083	0.439	0.067	0.443
	Sample D		**Sample E**		**Sample F**	
Temp. (°C)	1/time (min^{-1})	Drying rate (g/min)	1/time (min^{-1})	Drying rate (g/min)	1/time (min^{-1})	Drying rate (g/min)
58	0.065	0.287	0.061	0.290	0.056	0.302
80	0.100	0.462	0.083	0.431	0.077	0.426

Table 5. Drying rate of fabrics under different air temperature

The drying rate at the constant drying period increases with the rise of air temperature for all fabric samples.

3.2.4. Summary of the experimental findings

The period of constant drying as illustrated in Figs. 1 and 3 has constituted a large portion of the drying cycle. The moisture reduction rate at the period could be used as an indicator to show the properties of the fabric, and conditions of the impinging air. The experimental findings in Tables 3 – 5 have shown the performance of the drying process against the boundary conditions including fabric texture, density, thickness, air temperature and impinging velocity. It has been observed that the increase of air temperature and velocity will speed up the drying rate. The fabric properties could also affect the drying rate but not as much as the air properties. These findings could be useful in the setting up of analytical models to simulate each period of a fabric drying cycle.

4. Development of non-linear analytical models to simulate the drying of porous type fabrics

As mentioned in Section 2, the drying rate of porous type fabrics has a non-linear relationship with time at the falling drying period. Some inaccurate results will be found if the traditional linear heat transfer equations are applied because the heat transfer coefficient changes with the change of the moisture contents at the falling drying period. To ensure an accurate modeling of the drying process, the heat transfer coefficient should be adjustable corresponding to the diffusion properties in the forming of dry/wet regions as mentioned in Section 2.4. A non-linear model is therefore used to describe the process characteristics (Haghi, 2006; Moropoulou, 2005). The knitted and weaved fabrics studied in this research are considered porous type materials because they contain unidirectional pores. The randomly distributed pores give an environment to establish a diffusion process when portions of water dry up. It is clear that the moisture diffusion rate has a close relationship to the size and number of fabric pores. The studied models given in Section 4.6 will address these essential modeling parameters. The other fabric parameters including texture, density

and thickness that correlate to the drying rate will also be modeled by different modeling principles, and given in Sections 4.3 – 4.5.

4.1. Determination of the critical moisture content

The two periods of a fabric drying cycle as illustrated in Fig. 1 should be modeled separately. Traditional heat transfer equations could be used as modeling tools for the constant drying period, whilst, non-linear modeling equations should be considered when the moisture reduction rate varies with time in the falling drying period. The critical moisture content θ_k at the beginning of the falling drying period will be the separating point between the two periods. The finding of θ_k is given from the plotting of the normalized drying rate versus the moisture content in gram per gram of the dried fabric, see Fig. 4.

The moisture reduction rate $\dot{m}_n$ at the n^{th} period of a time interval Δt can be expressed as:

$$\dot{m}_n = \frac{m_n - m_{n+1}}{\Delta t} \text{ for the first time interval,} \tag{15}$$

$$\dot{m}_n = \frac{\left(m_{n-1} - m_n\right) + \left(m_n - m_{n+1}\right)}{2\Delta t} \text{for a time interval n } > \ 0 \tag{16}$$

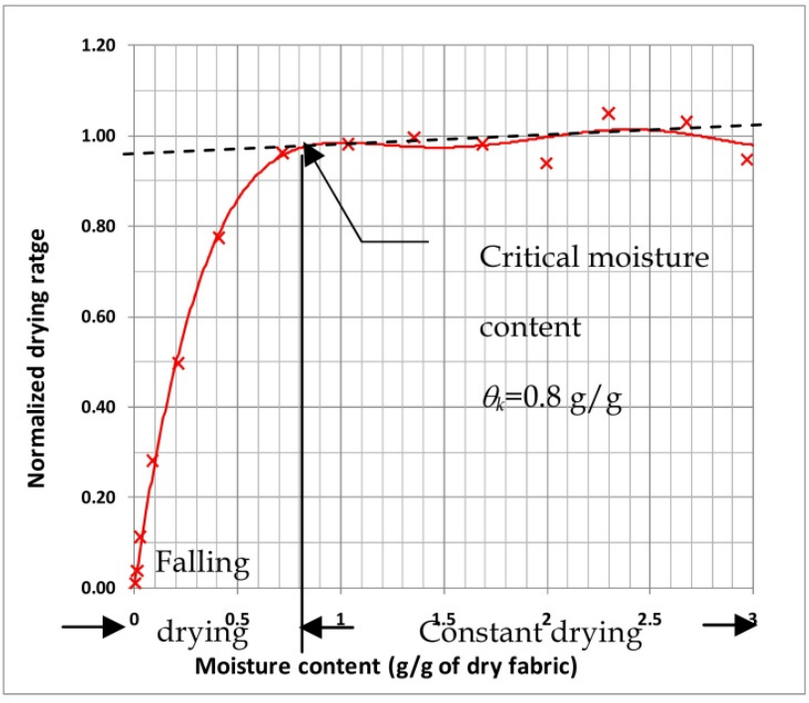

Figure 4. Plotting of normalized drying rate versus moisture content for fabric sample A

The critical moisture content θ_k can be identified from the curve as shown in Fig. 4 at the point of dramatic decrease of $\dot{m}_n$. The determined θ_k for fabric sample A under air setting condition 3 listed in Table 2 is 0.8 g/g. The testing results for other fabric samples under the same air setting condition are similar and listed in Table 6.

Fabric sample	Critical moisture content θ_k (g/g dry fabric weight)
A	0.8
B	0.7
C	0.8
D	0.8
E	0.7
F	0.7

Table 6. Critical moisture contents of the tested fabric samples

4.2. Using diffusion theories to model a fabric drying process

The boundary conditions for heat/mass transfer in the porous fabric have been discussed in Sections 2.2 to 2.5. However, they are not good enough to estimate the fabric moisture content during the drying process. It is necessary to have a further investigation to estimate the moisture content in individual period of drying. The authors have set-up a group of models based upon diffusion theories and Kowalski's (2003) boundary equations to simulate the moisture changing rate under various boundary conditions (Ip and Wan, 2011). The investigated drying models will be presented in differential forms to address the movement of moisture contents in fabric. The models are based on the principles of chemical diffusion mechanism to calculate the rate of moisture change (dM/dt) according to a set of modeling parameters empirically determined from drying cycles (Kowalski, 2000; Schlunder, 2004). Four non-linear analytical models, namely "Kinetics", "Diffusion", "Kinetics model based on the solutions of diffusion equations" and "Wet surface" have been developed, and the principles are given in the following sections.

4.3. First order kinetics model

Roberts and Tong (2003) have shown a successful result in the modeling of bread drying process using first order exponential equations. In their research, microwave was used as the drying agent, and the process has been assumed as isothermal. Unfortunately, the experiential setup is quite different from convective drying using impinging air in this study. It is therefore necessary to develop new modeling equations for porous type fabrics. Schlunder (2004) has stressed that the falling drying period should be considered as an isothermal process. First order exponential equations might be appropriate to describe the process, thus, the first model developed in this study is labeled as "First order kinetics model".

In the First order kinetics model, there is an assumption that the vaporization of water inside fabric can be described as a kinetic reaction motion of water molecules. The reaction rate is treated as the moisture reduction rate at the falling drying period. Thus, the water evaporation rate will correlate with the moisture content. The equation of the kinetic model is given as:

$$-\frac{dM}{dt} = kM^n \tag{17}$$

In Equation (17), M is the instant moisture content and $n = 1$ for the first order kinetics. If M_o is the initial moisture content at the beginning of the falling drying period, i.e. critical moisture content θ_k, the integration result of the differential form Equation (17) will be:

$$\frac{M}{M_o} = e^{-kt} \tag{18}$$

where k is the kinetic coefficient.

The testing results of moisture content as shown in Fig. 4 are further plotted in terms of drying cycle time t and given in Fig. 5. The red line in the figure represents the drying curve and the black line is the approximated drying rate at the constant drying period.

The kinetic coefficient k in Equation (18) at the falling drying period can be obtained by regenerating a new plotting from the results illustrated in Fig. 5. The ratio of M/M_o in the equation shows an exponential relationship with $-kt$. It can be converted into a linear relationship by applying logarithm for both sides of Equation (18). Fig. 6 shows a plotted graph of $\ln(M/Mo)$ versus the drying cycle time from the experimental records in Fig. 5.

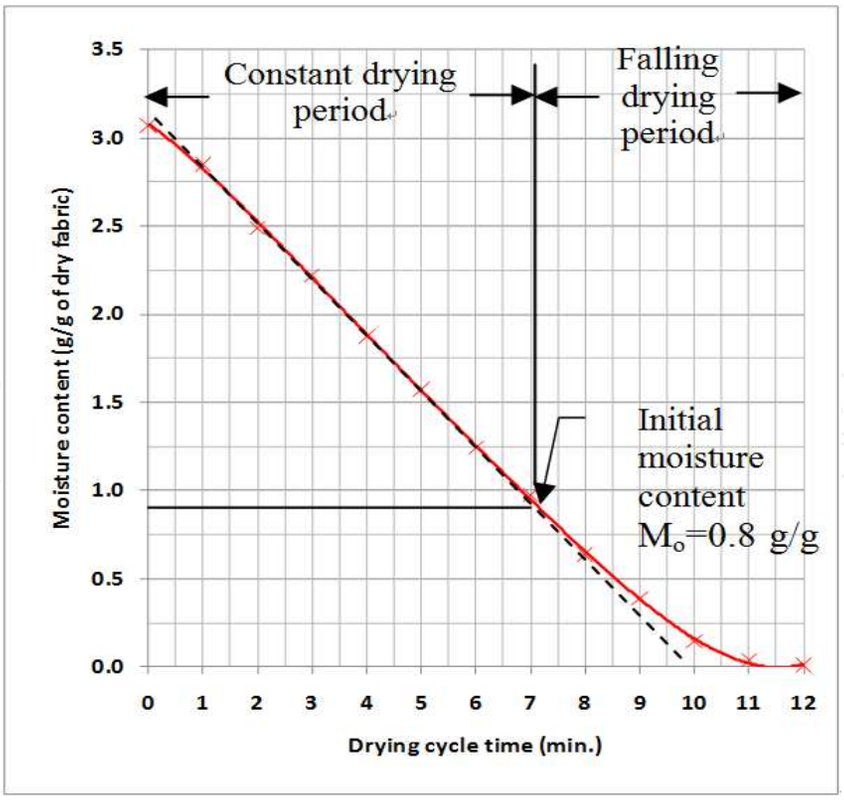

Figure 5. Experimental records of the drying of fabric sample A

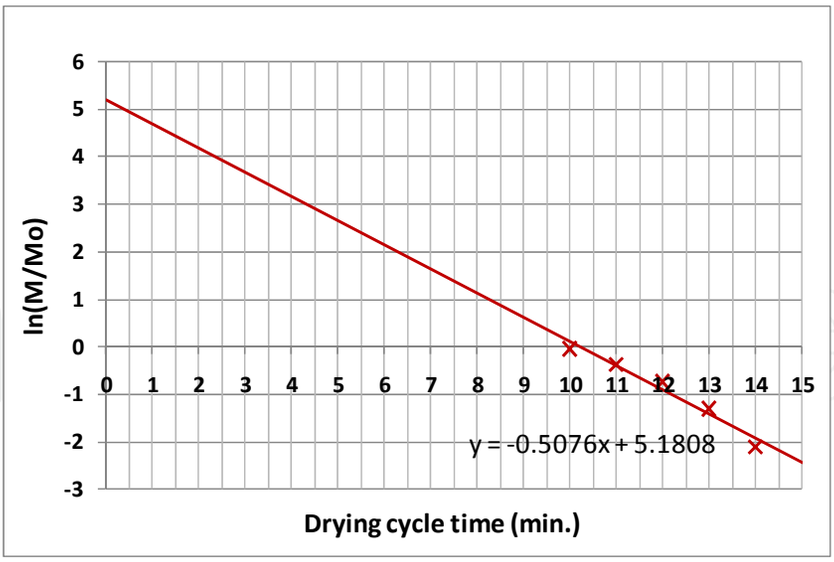

Figure 6. Determination of kinetic coefficient k for fabric sample A

A graphical method to determine the kinetic coefficient k is to measure the slope of the fitted line in Fig. 6. The slope is measured as -0.5076 that will be the tested fabric kinetic coefficient. An alternative method to determine k is to modify Equation (18) using Arrhenius relationship (Roberts and Srikiatden, 2005). It is a common method to correlate rate constant with reaction temperature T for kinetics reactions in chemistry. The Arrhenius form of equation in terms of k and T is:

$$k = Ae^{-E_a/RT} \tag{19}$$

where E_a is the activation energy, R is the universal gas constant at 8.314×10^{-3} kJ/mol K and A is a constant. Equation (19) gives the relationship of kinetic coefficient k in terms of air temperature T only, and does not include the impinging velocity V. However, V is also a key factor in the drying process and its effect could be empirically determined using linear regression methods. The regression equation for the calculation of k from the Arrhenius relationship in Equation (19) is given by taking natural algorithm of the equation.

$$\ln k = \frac{-E_a}{R}\frac{1}{T} + \ln A \tag{20}$$

A in the Arrhenius equation means reaction per time and is correlated to the impinging velocity in the studied drying models. Thus, the First order kinetics model in Arrhenius form can be written in terms of T and V to give:

$$\ln k = a + b\frac{1}{T} + c\ln V \tag{21}$$

If the Arrhenius relationship is applied to describe a fabric drying process, a plotting of ln k versus $1/T$ will give a straight line. The slope and intercept of the line are used to determine the correlation constants of E_a and b as given in Equations (20) and (21). The kinetic

coefficient k of the fabric sample A calculated from Equation (19) under the air setting conditions listed in Table 2 are given in Table 7, and the corresponding values of ln k, $1/T$ and ln V determined from Equation (21) are listed in Table 8.

Setting condition	AIR TEMPERATURE (K)	Impinging velocity (m/s)	k^*	k
1	353.0	1.48	0.5295	0.5198
2	354.5	1.45	0.5818	0.5230
3	359.5	1.43	0.5076	0.5336
4	327.0	1.10	0.5297	0.4634
5	328.5	1.15	0.5494	0.4667
6	327.0	1.02	0.5537	0.4634
7	330.0	1.41	0.3589	0.4699
8	331.0	1.46	0.3568	0.4722

Table 7. The calculated kinetic coefficients from experiments and Arrhenius equation for fabric sample A (k^* from experiential results, k from Arrhenius equation)

Setting condition	ln k	$1/T$ (K^{-1})	ln V (m/s)
1	-0.6358	0.0028	0.3920
2	-0.5416	0.0028	0.3716
3	-0.6781	0.0028	0.3577
4	-0.6354	0.0031	0.0953
5	-0.5989	0.0030	0.1398
6	-0.5911	0.0031	0.0198
7	-1.0247	0.0030	0.3436
8	-1.0306	0.0030	0.3784

Table 8. The calculated correlation constants for the tested fabric sample A

Fig. 7 illustrates the plotting of ln k versus $1/T$ from data in Table 8. Results from the plotting were used to calculate the activation energy E_a and A as given in Equation (20).

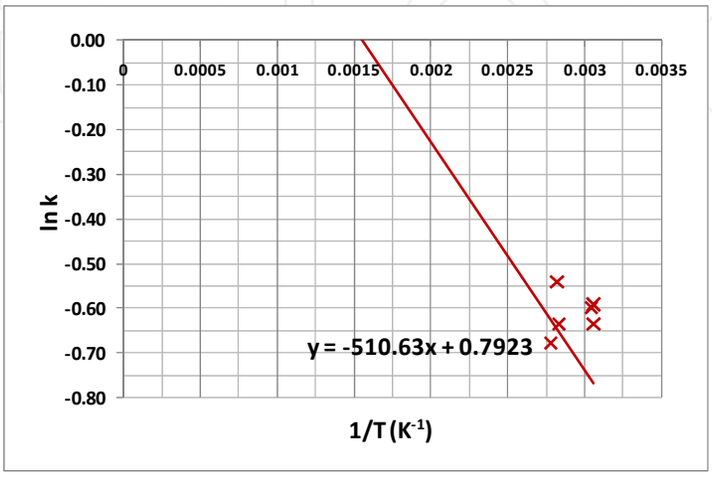

Figure 7. The plotting of ln k versus $1/T$ for fabric A under various air setting conditions

The calculated values for E_a and A are 4.2454 kJ/mole and 2.2085 respectively given from Fig. 7. The final form of the Arrhenius equation for fabric sample A will be given as:

$$\ln k = -510.63\frac{1}{T} + 0.7923 \tag{22}$$

Experimental results listed in Table 8 can be further used to determine the coefficients of *a*, *b* and *c* as given in Equation (21) by linear regression methods (Cohen, 2003). The regression results produced from MicroSoft Excel for fabric sample A are given in Fig. 8.

SUMMARY OUTPUT				
Regression Statistics				
Multiple R	0.8912112			
R Square	0.7942575			
Adjusted R Square	0.7256766			
Standard Error	0.1058416			
Observations	9			
ANOVA				
	df	*SS*	*MS*	*F*
Regression	2	0.259478294	0.129739	11.58133
Residual	6	0.067214622	0.011202	
Total	8	0.326692916		
	Coefficients	*Standard Error*	*t Stat*	*P-value*
Intercept	5.5354099	1.333590724	4.150756	0.006006
1/T[k]	-1974.7449	429.2456499	-4.6005	0.00369
lnV	-1.5207901	0.359403041	-4.23143	0.005491

Figure 8. Regression table for fabric sample A determined from the First order kinetics model

Using results from the regression table, the model equation is given as:

$$\ln k = 5.535 - 1974.7\left(\frac{1}{T}\right) - 1.521\ln V, \text{where } a = 5.535, b = -1974.7 \text{ and } c = -1.521 \tag{23}$$

Fabric sample	a	b	c
A	5.535	-1974.7	-1.521
B	5.740	-1993.9	-1.210
C	3.714	-1476.9	-0.911
D	4.430	-1584.6	-1.276
E	5.580	-2054.5	-0.494
F	6.087	-2223.7	-0.280

Table 9. Regression results of the tested fabric samples

Table 9 lists the regression results of all the fabric samples. A comparison of the differences of *k* determined from Arrhenius equation and regression model for fabric sample A is listed in Table 10.

Setting	AIR TEMP. (°C)	Velocity (m/s)	*k1*	*k2*	*k1* Dev. (%)	*k2* Dev. (%)
1	80.0	1.48	0.5198	0.5195	1.83	1.90
2	81.5	1.45	0.5230	0.5487	10.10	5.68
3	86.5	1.43	0.5336	0.6056	5.12	19.30
4	54.0	1.10	0.4634	0.5227	12.52	1.32
5	55.5	1.15	0.4667	0.5022	15.06	8.59
6	54.0	1.02	0.4634	0.5863	16.32	5.89
7	57.0	1.41	0.4699	0.3786	30.95	5.50
8	58.0	1.46	0.4722	0.3656	32.34	2.48
		Average	0.4890	0.5037	15.53	6.333

k1 is calculated from Arrhenius equation (Equation 19), *k2* is calculated from regression model (Equation 21)

Table 10. Comparison of kinetic coefficient determined from Arrhenius equation and regression model for fabric sample A

The deviations of *k* for Arrhenius and regression models listed in Table 10 are calculated based on the results obtained from experiments listed in Table 7. The deviations calculated from regression model are much less than Arrhenius equation. The impinging velocity may have been considered in the regression model. Further study about the discrepancy of the modeling results between the regression model and the experimental records was performed.

The red curve illustrated in Fig. 9 is the modeled drying cycle obtained from the regression model for fabric sample A in the falling drying period with a kinetic coefficient *k* at 0.5037. Discrepancies have been found in comparison with the blue drying curve obtained from experiments. The average discrepancy and standard deviation of the comparison are 14.0139% and 7.8028% respectively.

In conclusion, the falling drying period in a fabric drying cycle can be modeled by the First order kinetics model using an exponential function. A coefficient *k* for the exponential function can be experimentally determined to model the drying characteristics under various air setting conditions. The coefficient can also be numerically determined from the regression model using air temperature and impinging velocity as the boundary conditions. It has a further relationship to the fabric density and thickness as illustrated in Fig. 10 other than temperature and velocity. Table 11 lists *k* determined from the regression model for all the fabric samples. It has been found that *k* decreases with the increase of fabric density and thickness. This relationship could be useful in the estimation of the drying cycle time for the fabrics with different thickness and density.

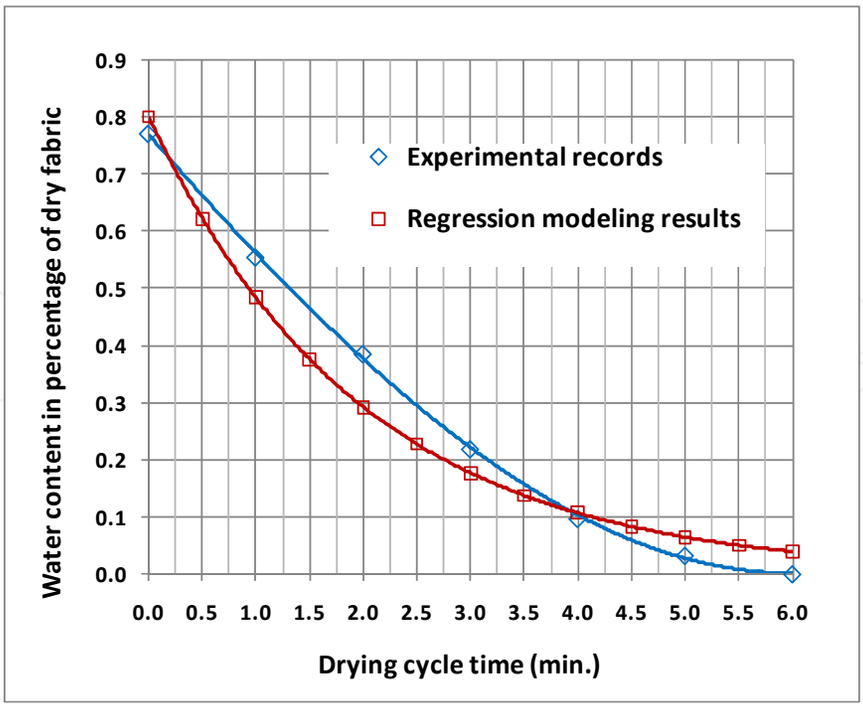

Figure 9. Comparison of experimental records and regression modeling results for fabric sample A

Fabric sample	Density (g/m³)	Thickness (mm)	*k*
A	224	0.6594	0.5037
B	148	0.4363	0.6328
C	271	0.7769	0.4136
D	182	0.5638	0.5607
E	193	0.5025	0.5469
F	200	0.6188	0.5869

Table 11. The fabric kinetic coefficient *k* determined from the regression model

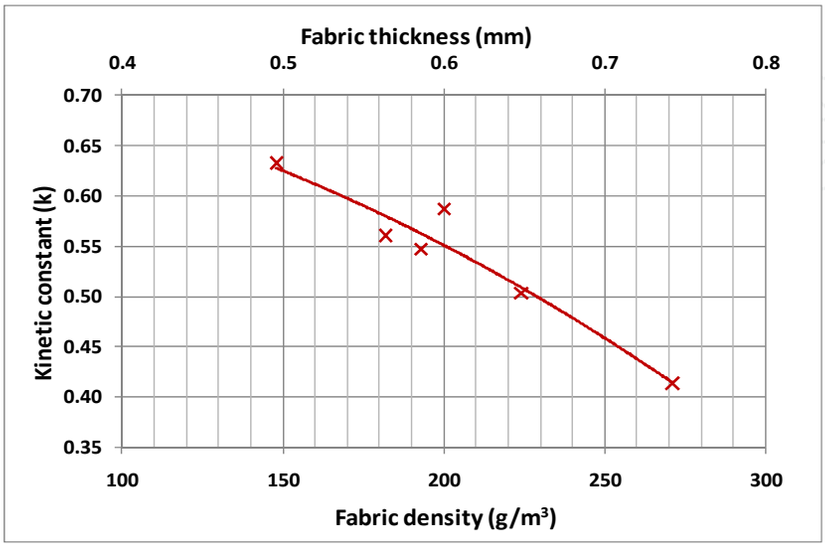

Figure 10. Relationship of *k* to the fabric density and thickness

4.4. Diffusion model

Most of the Diffusion models presenting the change of moisture content have been based upon Fick's law (Ramaswamy and Nieuwenhuijzen, 2002). The Fick's first law states the diffusion flux flowing from the regions of higher concentration to lower concentration obeying a magnitude proportional relationship to the concentration gradient. The one dimensional Fick's first law in differential form is given as:

$$J = -D\frac{\partial \phi}{\partial x} \tag{24}$$

where J is the diffusion flux in $m^{-2}s^{-1}$, D is the effective diffusion coefficient in $m^2\ s^{-1}$, $\emptyset$ is the concentration in m^{-3} and x is a linear distance in m. The Fick's second law given in Equation (25) shows the rate of concentration change. It is given by the derivative of Equation (24), with the assumption of D as a constant. The Fick's second law has been used commonly to simulate the drying process of agricultural products (Khazaei et al., 2008), such as seeds and grains.

$$\frac{\partial \phi}{\partial t} = D\frac{\partial^2 \phi}{\partial x^2} \tag{25}$$

If the Fick's second law is applied to model the process of drying porous fabric, the fabric will be considered as an infinite thin slab and dried from one direction. If heat transfer from the surrounding to the fabric is negligible, the integration result from Equation (25) will give the Diffusion model. The model equation given in Equation (26) is in terms of moisture content M, fabric thickness L, effective diffusion coefficient D and the drying cycle time t.

$$\frac{M}{M_o} = \frac{8}{\pi^2}\exp\left(-\frac{\pi^2 Dt}{4L^2}\right) \tag{26}$$

The Diffusion equation is similar to Equation (18) of the First order kinetics model. The only difference between the two model equations is the fabric thickness L included in the Diffusion model. As the same as in the First order kinetics model, the effective diffusion coefficient D in Equation (26) can be acquired from the plotting of ln (M/M_o) versus t as illustrated in Fig. 6. Equation (27) is obtained when a logarithm is applied to both sides of Equation (26).

$$\ln\frac{M}{M_o} = \left(-\frac{\pi^2 D}{4L^2}\right)t - 0.21 \tag{27}$$

The slope of the fitted straight line in Fig. 6 is -0.5076 for fabric sample A with a thickness of 0.6594 mm. D is then calculated by substituting the slope and L back to Equation (27), and the estimated value is 8.945×10^{-8}. The equation form of the Diffusion model and the First order kinetics is similar, D in the Diffusion model can be therefore calculated using the regression model. The Diffusion model in regression form is given in Equation (28).

$$\ln D = a + b\frac{1}{T} + c\ln V \tag{28}$$

Using information in Table 8 to determine the constants of *a, b* and *c*. The determined regression model equation for fabric sample A is given as:

$$\ln D = 20.879 - 12070.75\frac{1}{T} - 2.173\ln V \tag{29}$$

The regression results for all the fabric samples are listed in Table 12.

Fabric sample	a	b	c
A	20.88	-12070.75	2.173
B	10.59	-2006.16	1.215
C	11.43	-1495.8	0.9718
D	11.374	-1601.97	1.277
E	10.578	-1895.1	0.526
F	10.08	-2201.5	0.242

Table 12. Regression results of all the fabric samples modeled by Diffusion model

The effective diffusion coefficient *D* for fabric sample A calculated from various air setting conditions are listed in Table 13.

Setting	AIR TEMP. (°C)	Impinging velocity (m/s)	Effective diffusion coeff. *D*
1	80.0	1.48	7.03023×10^{-7}
2	81.5	1.45	8.49438×10^{-7}
3	86.5	1.43	1.40575×10^{-6}
4	54.0	1.10	8.83487×10^{-8}
5	55.5	1.15	9.49414×10^{-8}
6	54.0	1.02	1.04100×10^{-7}
7	57.0	1.41	7.20528×10^{-8}
8	58.0	1.46	7.46037×10^{-8}
		Average	4.24032×10^{-7}

Table 13. Effective diffusion coefficient *D* for fabric sample A under various conditions

Fig. 11 illustrates a comparison between the experiential records and the modeling results from regression model using D at 4.24032×10^{-7}.

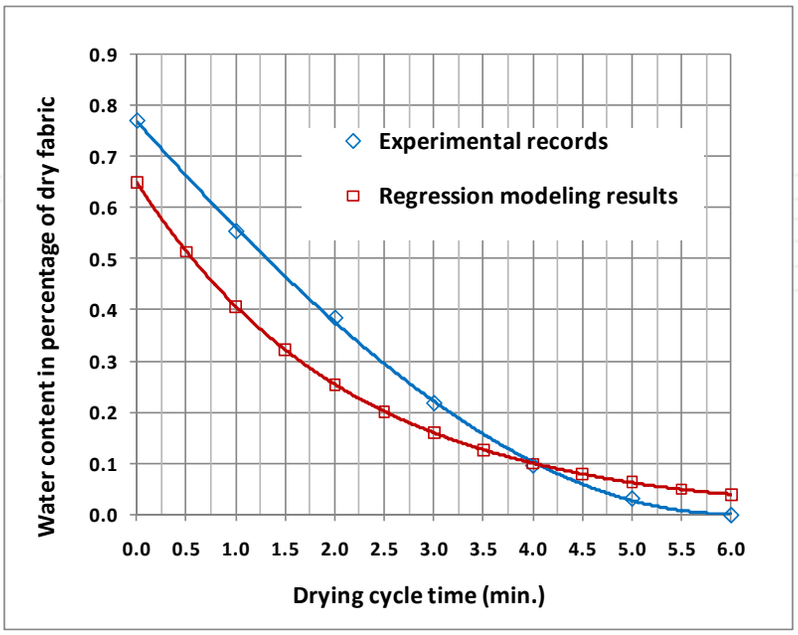

Figure 11. A comparison of regression results from Diffusion model and experimental records for fabric sample A

The Diffusion model has been applied to model each of the drying cycle for all fabric samples, the discrepancies between the modeling results and records from experiments are listed in Table 14.

Fabric sample	A	B	C	D	E	F
Discrepancy (%)	76.63	42.86	49.03	44.44	48.35	43.34

Table 14. Discrepancies of a comparison of Diffusion model and records of experiments

4.5. Kinetics model based on the solutions of diffusion equations

Fick's second law for diffusion applications is commonly used to simulate mass transfer process in convective drying. However, the exponential term in Equation (26) causes a restriction to the Diffusion model be applied in the falling drying period. A separate modeling process is needed to describe the constant drying period for completed modeling of a drying cycle. Efremov (1998, 2002) has proposed a mathematical solution to solve the Frick's law using integral error functions:

$$\frac{m}{m_o} = 1 - erf\frac{x}{2\sqrt{Dt}} \tag{30}$$

$$\frac{m}{m_o} = 1 - N_o\frac{t}{m_o} \tag{31}$$

where m is the moisture removal rate, m_o is the initial moisture removal rate, N_o is the drying rate at the constant drying period and x is the fabric thickness. Substituting the boundary conditions of $t = 0$ and $t = t_f$ for a drying cycle at the starting and ending points, a kinetics model equation developed from the diffusion model is given as:

$$\frac{m}{m_o} = 1 - N_o \frac{t}{w_o} + \frac{N_o \sigma \sqrt{\pi}}{2 w_o} \left(1 - erf \frac{t_f - t}{\sigma} \right) \tag{32}$$

where σ is a characteristic drying time and expressed as:

$$\sigma = 2 \frac{N_o t_f - m_o}{N_o \sqrt{\pi}} \tag{33}$$

The first and second terms in the right-hand-side of Equation (32) represent the characteristics in the constant drying period, and the third term represents the falling drying period. The new kinetics equation consists of two modeling sections to describe the linear and non-linear parts of a drying process. The drying rate at constant drying period N_o and the drying cycle time t_f are needed to be predetermined when Equation (32) is applied. N_o is the slope of the dotted line as shown in Fig. 5, they are given in Table 15.

Setting condition	**Drying rate at constant drying period of the fabric samples (g/s)**					
	A	**B**	**C**	**D**	**E**	**F**
1	0.0069	0.0073	0.0074	0.0077	0.0072	0.0071
2	0.0069	0.0079	0.0083	0.0080	0.0084	0.0071
3	0.0065	0.0067	0.0069	0.0069	0.0070	0.0065
4	0.0068	0.0064	0.0065	0.0066	0.0051	0.0054
5	0.0066	0.0065	0.0072	0.0066	0.0074	0.0074
6	0.0063	0.0065	0.0066	0.0066	0.0058	0.0064
7	0.0047	0.0046	0.0051	0.0047	0.0048	0.0051
8	0.0047	0.0047	0.0048	0.0048	0.0048	0.0050
Average	0.00618	0.00633	0.00660	0.00649	0.00631	0.00625

Table 15. The drying rate at constant drying period of the fabric samples under different air setting conditions

The drying rate at constant drying period N_o listed in Table 15 for each fabric sample and their corresponding drying cycle time t_f are employed to assist the simulation of entire drying process. Equation (32) is the modeling tool to calculate the moisture removal rate m from t_o to t_f. The red curve in Fig. 12 illustrates the modeling results determined from Equation (32). The values for N_o and t_f are 0.00618 and 15 min. respectively. The modeling process has been repeated for the falling drying period using the final term of Equation (32), and the results are given in Fig. 13.

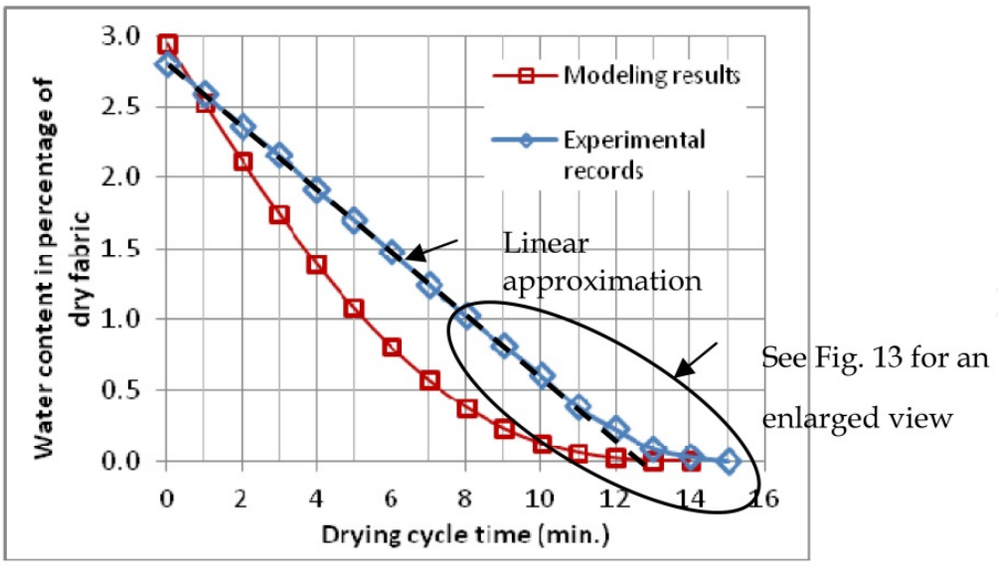

Figure 12. A comparison of modeling results from Equation (32) and testing records of a complete drying cycle for fabric sample A under air setting condition 3

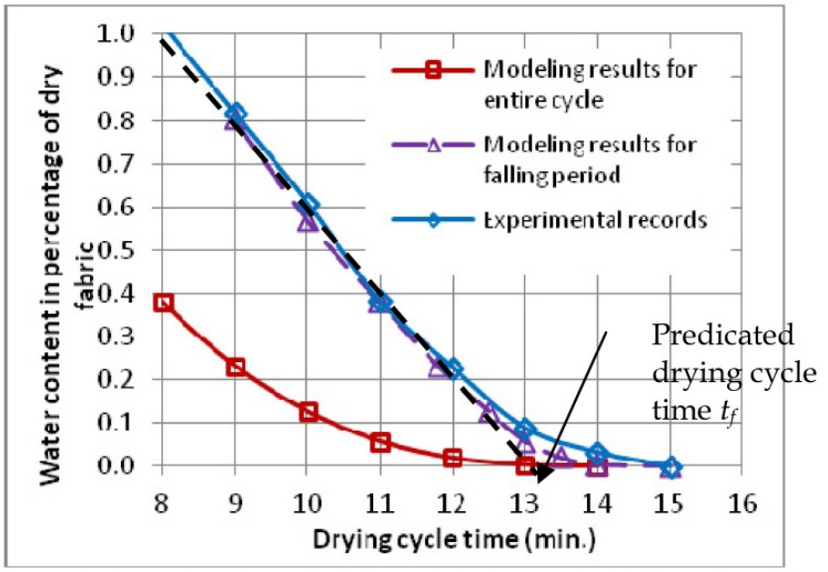

Figure 13. A comparison of modeling results from Equation (32) for the falling drying period and testing records of fabric sample A under air setting condition 3

Tables 16 and 17 list the discrepancies of the two modeling results from Figs. 12 and 13.

Fabric sample	A	B	C	D	E	F
Discrepancy (%)	41.17	30.25	40.53	30.21	36.63	38.06

Table 16. Discrepancies between the tests and modeling results for entire drying cycle

Fabric sample	A	B	C	D	E	F
Discrepancy (%)	8.70	7.92	10.12	11.69	8.87	7.15

Table 17. Discrepancies between the tests and modeling results at the falling drying period

4.6. Wet surface model

The fourth analytical model, Wet surface, was proposed by Schlunder (1988, 2004). He has proved that the remaining moisture in porous materials would be 20 to 30 % of the saturated moisture content at the initial stage when a drying process reaches the critical moisture stage. The material surface is unlikely to be fully wetted at this low moisture content condition. The Wet surface model is therefore designed to address the characteristics of the partially wet surface. The drying rate $\dot{M}_v$ is modeled directly in contrast with the calculation of the moisture content M required in the previous models. The Wet surface equation is given as:

$$\frac{\dot{M}_v}{\dot{M}_{vI}} = \frac{1}{1+\phi} \tag{34}$$

$$\phi = \frac{2r}{\pi\varepsilon}\sqrt{\frac{\pi}{4\varphi}}\left(\sqrt{\frac{\pi}{4\varphi}} - 1\right) \tag{35}$$

$\dot{M}_v$ is the instant drying rate and $\dot{M}_{vI}$ is initial drying rate when the fabric surface is fully wetted, r is pore size, ε is viscous sub-layer thickness and φ is the fraction of a wet surface. It is assumed that the wet surface fraction φ is proportional to a ratio of moisture content θ to the critical moisture content θ_c in the falling drying period, thus the Equation (35) is rewritten as:

$$\phi = \frac{2r}{\pi\varepsilon}\sqrt{\frac{\pi}{4\frac{\theta}{\theta_c}}}\left(\sqrt{\frac{\pi}{4\frac{\theta}{\theta_c}}} - 1\right) \tag{36}$$

The results of converting Equation (36) from the critical moisture content θ_c to the final moisture content give an expression as:

$$\theta - \theta_c + \frac{r}{2\varepsilon}\theta_c \ln\frac{\theta}{\theta_c} - \frac{2r}{\sqrt{\pi}\varepsilon}\sqrt{\theta_c\theta} + \frac{2r}{\sqrt{\pi}\varepsilon}\theta_c = \dot{M}_{vI}t \tag{37}$$

In Equation (37), the parameters for fabric drying modeling are the initial drying rate $\dot{M}_{vI}$, critical moisture content θ_c, pore size r and viscous sub-layer thicknessε. In fact, $\dot{M}_{vI}$ and θ_c can be experimentally determined as discussed in Section 4.1. The viscous sub-layer thickness ε is in terms of thermal conductivity of air c and heat transfer coefficient U, they are given as:

$$\varepsilon = c/U \tag{38}$$

$$U = \frac{\lambda N_o}{A\left(T_h - T_{SL}\right)} \tag{39}$$

where λ is the latent heat of vaporization, A is the fabric surface area, T_h and T_{SL} are temperature of the drying air and the temperature at saturated condition respectively. The values of λ, T_{SL} and c can be found from engineering handbooks. Table 18 lists the calculated ε for the fabric sample A from Equations (38) and (39).

Setting condition	N_o (g/s)	T_h (K)	T_{SL} (K)	λ (J/g)	U (W/m²K)	c (W/mK)	ε (mm)
1	0.0069	353.0	301	2310	30.79	0.028	0.91
2	0.0077	354.5	301	2304	33.29	0.028	0.84
3	0.0065	359.5	302	2291	25.70	0.028	1.09
4	0.0068	327.0	293	2372	47.35	0.028	0.59
5	0.0066	328.5	294	2372	45.32	0.028	0.62
6	0.0063	327.0	293	2372	43.89	0.028	0.64
7	0.0047	330.0	294	2366	31.04	0.028	0.90
8	0.0047	331.0	295	2366	30.75	0.028	0.91
						Average	0.8125

Table 18. The viscous sub-layer thickness ε for the fabric sample A

The final parameter to be determined for Equation (37) is the fabric pore size r. The pore size can be measured under microscope but it is not practical to determine through microscopic images. A better way to acquire the pore size can be done by graphical methods. Fig. 14 shows the plotting of the predicted drying rate from the Wet surface model versus the moisture reduction rate experimentally determined from Equation (15).

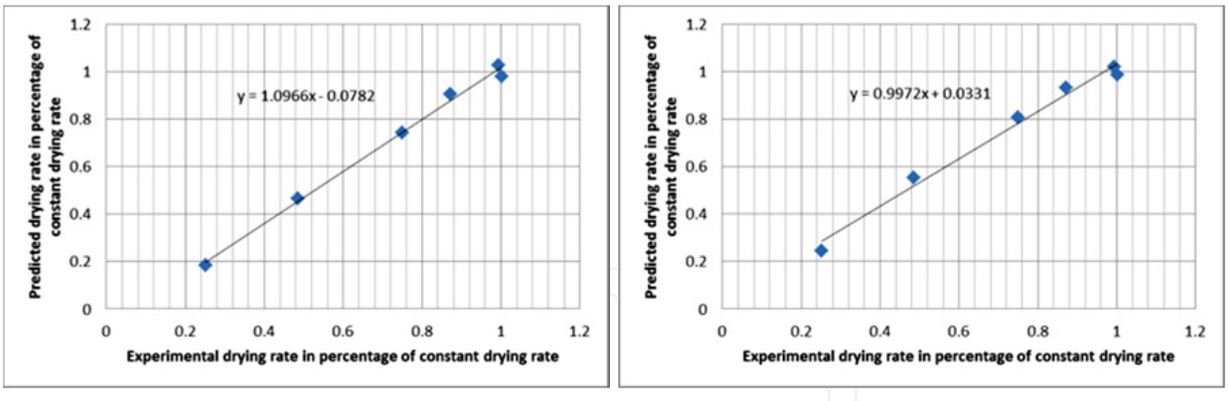

(a) (b)

Figure 14. Relationship of predicted drying rate to experimentally determined drying rate for the assigned pore size r at (a) 0.5 mm and (b) 0.3478 mm for fabric sample A

The fitted line in Fig. 14(a) shows the results from an assigned pore size of 0.5 mm. Results from the plotting have shown that the slope of the fitted line is not a unity, and the y-intercept does not meet the origin. As a result, the calculated viscous sub-layer thickness ε from the pore size does not consist with the calculated value as listed in Table 18. Thus, a new assignment of 0.3478 mm was used to create another plotting. The new fitted line as

illustrated in Fig. 14(b) is much closer to unity slope and zero y-intercept conditions. The new pore size could be used as the modeling parameter in the Wet surface model.

Table 19 lists the determined pore sizes for other fabric samples. The calculated pore sizes for each fabric sample are then substituted into Equation (37) to determine the drying rate $\dot{M}_v$. A comparison of the discrepancies between the modeled drying rate and recorded data from experimental tests for fabric sample A under the air setting condition 3 is given in Fig. 15.

	Fabric sample					
Setting condition	**A**	**B**	**C**	**D**	**E**	**F**
1	0.40	0.61	0.19	0.31	0.46	0.36
2	0.40	0.55	0.35	0.70	0.40	0.45
3	0.35	0.40	0.55	0.31	0.21	1.55
4	0.16	0.23	0.22	0.25	0.20	0.50
5	0.19	0.31	0.22	0.40	0.37	0.35
6	0.33	0.07	0.49	0.40	0.37	0.44
7	0.40	1.10	0.60	0.31	0.43	0.55
8	0.55	0.53	0.49	1.50	1.10	1.20
Average	0.3478	0.4750	0.3888	0.5225	0.4425	0.6750

Table 19. The determined pore size in mm for the tested fabric samples

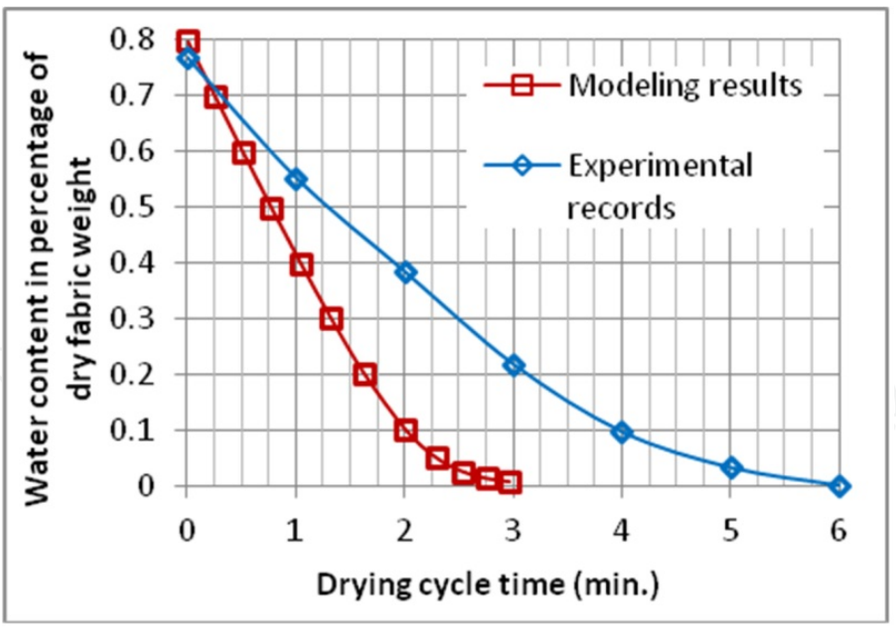

Figure 15. A comparison of the modeling results using Equation (37) and testing records for fabric sample A under test setting 3 for the falling drying period

The findings given in Fig. 15 have shown that the Wet surface model could not produce an accurate modeling result as the measured discrepancy is 77.53 % based upon the experimental records.

5. A performance evaluation of the studied models

The performance of the studied analytical models for the modeling of porous fabric drying process should be reviewed. The percentage of discrepancies from each modeling results in comparison with the experimental records are summarized in Table 20. It is made clear that the Kinetics model based on the solutions of diffusion equations has produced the best performance. The First order kinetics model has provided a better performance than the Diffusion model, and the Wet surface model has given the largest discrepancy from the statistical records listed in Table 20.

Model	Fabric sample						
	A	B	C	D	E	F	Average
First order kinetics	42.39	34.69	38.74	34.21	42.25	37.11	38.23
Diffusion	76.63	42.86	49.03	44.44	48.35	43.34	50.77
Kinetics based on the solutions of diffusion equations	8.70	7.92	10.12	11.69	8.87	7.15	9.08
Wet surface	77.53	37.47	93.50	56.00	69.87	64.02	66.40

Table 20. Summary of performance evaluation of the studied models

The findings have shown that the Kinetics model based on the solutions of diffusion equations could be the best one in the simulation of a porous fabric drying process among the others. The required condition for the model is to have a predictable drying cycle time t_f that could be obtained by a linear approximation of the experimentally determined drying curve as shown in Fig. 13. First order kinetics model has also produced a good performance in comparison with the Diffusion and Wet surface model. An empirically determined kinetic coefficient k is only needed for the modeling process, and the coefficient is highly correlated to temperature and impinging velocity of air. A less accurate modeling result observed from the Diffusion model is that a fabric thickness L is needed for the model equation. A significant change of the exponential index in Equation (26) would cause a large discrepancy in the modeling result if the thickness is inaccurately defined. It is understandable that the complexity of finding the pore size would cause unavoidable errors in the Wet surface model. To design experimental strategies determining the pore size to improve the model performance is some further work.

6. Conclusion

The principles of water mass movement due to phase change in the drying of porous fabrics have been studied. The boundary equations for mass transfer between water, vapor and air were used to support the establishing a new set of drying models using diffusion theories. Experiments were done to find information for the determination of the modeling parameters. The performance of the developed models has been evaluated. Among the four models, the Kinetics model based on the solutions of diffusion equations has produced the best performance. In the real life applications, they could act as a mathematical tool to assist

a precise estimation of the moisture content in fabric drying or heat setting process under various processing conditions. Further work has been started to apply the developed drying models in the design of garment setting machines for clothing industry.

Author details

Ralph Wai Lam Ip and Elvis Iok Cheong Wan
Department of Mechanical Engineering, The University of Hong Kong, Pokfulam, Hong Kong SAR

7. References

Cohen, J., Cohen P., West, S.G., & Aiken, L.S. (2003). *Applied Multiple Regression/Correlation Analysis for the Behavioral Sciences.* (2nd ed.): Lawrence Erlbaum Associates, Hillsdale, NJ

Efremov, G.I. (1998). Kinetics of Convective Drying of Fibre Materials Based on Solution of a Diffusion Equation. *Fibre Chemistry*, Vol. 30, No. 6, pp. 417-422

Efremov, G.I. (2002). Drying Kinetics Derived from Diffusion Equation with Flux-Type Boundary Conditions. *Drying Technology*, Vol. 20, No. 1, pp. 55-66

Haghi, A.K. (2006). Transport Phenomena in Porous Media: A Review. *Theoretical Foundations of Chemical Engineering*. Vol. 40, No. 1, pp. 14-26

Ip, R.W.L. & Wan, I.C. (2011). New Use Heat Transfer Theories for the Design of Heat Setting Machines for Precise Post-Treatment of Dyed Fabrics. *Journal Defect and Diffusion Forum*, Vols. 312-315, pp. 748-751

Khazaei, J.; Chegini, G.R. & Bakhshiani, M. (2008). A Novel Alternative Method for Modeling the Effects of Air Temperature and Slice Thickness on Quality and Drying Kinetics of Tomato Slices: Superposition Technique. *Drying Technology*, Vol. 26, No. 6, pp. 759-775

Kowalski, S.J. (2000). Toward a Thermodynamics and Mechanics of Drying Processes. *Chemical Engineering Science*, Vol. 55, No. 7, pp. 1289-1304.

Kowalski, S.J. (2003). *Thermomechanics of Drying Processes*, Springer, ISBN 3-540-00412-2, Berlin, Germany

Kowalski, S.J.; Musielak, G. & Banaszak, J. (2007). Experimental Validation of the Heat and Mass Transfer Model for Convective Drying. *Drying Technology*, Vol. 25, No. 1-3, pp. 107-121

Moropoulou, A. (2005). Drying Kinetics of Some Building Materials. *Brazilian Journal of Chemical Engineering*, Vol. 22, No. 2, pp. 203-208

Ramaswamy, H.S. and van Nieuwenhuijzen, N.H. (2002). Evaluation and Modeling of Two-Stage Osmo-Convective Drying of Apple Slices. *Drying Technology*, Vol. 20, No. 3, pp. 651-667

Roberts, J.S. and Srikiatden, J. (2005). Moisture Loss Kinetics of Apple During Convective Hot Air and Isothermal Drying. *International Journal of Food Properties*, Vol. 8, No. 3, pp. 493-512

Roberts, J.S. & Tong,C.H. (2003). Drying Kinetics of Hygroscopic Porous Materials under Isothermal Conditions and the Use of a First-Order Reaction Kinetic Model for Predicting Drying. *International Journal of Food Properties.* Vol. 6, No. 3, p. 355-367.

Schlunder, E.U. (1988). On the Mechanism of the Constant Drying Rate Period and Its Relevance to Diffusion Controlled Catalytic Gas-Phase Reactions. *Chemical Engineering Science*, Vol. 43, No. 10, pp. 2685-2688

Schlunder, E.U. (2004). Drying of Porous Material during the Constant and the Falling Rate Period: A Critical Review of Existing Hypotheses. *Drying Technology*, Vol. 22, No. 6, pp. 1517-1532